archives
of thermodynamics
Vol. **41**(2020), No. 1, 31–66
DOI: 10.24425/ather.2020.132949

Magneto-thermoelastic problem in the context of four theories under influence of laser pulse and gravity field

SAYED ABO-DAHAB[a,b]
ABDELMOOTY ABD-ALLA [*c]
ABDELKALK ALQARNI[b]

[a] Mathematics Department, Faculty of Science, Taif University 888, Saudi Arabia

[b] Mathematics Department, Faculty of Science, South Valley University, Qena 83523, Egypt

[c] Mathematics Department, Faculty of Science, Sohag University, Egypt

Abstract The paper is devoted to study the effect of gravity, magnetic field and laser pulse on the general model of the equations of generalized thermoelasticity for a homogeneous isotropic elastic half-space. The formulation is applied under four theories of generalized thermoelasticity: the coupled theory, Lord-Schulman theory, Green-Lindsay theory as well as Green-Naghdi theory. By employing normal mode analysis, the analytical expressions for the displacement components, temperature and the (mechanical and Maxwell's) stresses distribution are obtained in the physical domain. These expressions are also calculated numerically and corresponding graphs are plotted to illustrate and compare the theoretical results. The effect of gravity, magnetic field and laser pulse are also studied and displayed graphically to show the physical meaning of the phenomena. A comparison has been made between the present results and the results obtained by the others. The results indicate that the effects of magnetic field, laser pulse and gravity field are very pronounced.

[*]Corresponding Author. Email: mohmrr@yahoo.com

Keywords: Generalized thermoelasticity; Gravity; Laser pulse; Magnetic field; Half-Space

1 Introduction

The subject of generalized thermoelasticity has drawn the attention of researchers due to its relevance in many practical applications. The generalized thermoelasticity theories involve hyperbolic type governing equations and admit finite speed of thermal signals. The extensive literature on the topic is now available and we can only mention a few recent interesting investigations [1–7]. Generalized theories of thermoelasticity have been developed to overcome the infinite propagation speed of thermal signals predicted by the classical coupled dynamical theory of thermoelasticity [8]. The non-classical theories of thermoelasticity, so-called generalized thermoelasticity, have been developed to remove the paradox of the physically impossible phenomenon of infinite velocity of thermal signals in the conventional coupled thermoelasticity, Lord-Shulman theory [9] and Green-Lindsay theory [10]. In the 1990s, Green and Naghdi (G-N) have formulated three models (I, II, III) of thermoelasticity for homogeneous and isotropic material [11]. The model I of G-N theory after linearization reduces to the classical thermoelasticity theory. The model II of G-N theory [12] does not allow dissipation of the thermoelastic energy. In this model, the constitutive equations are derived by starting with the reduced energy equation and by including the thermal displacement gradient among the constitutive variables. The effect of gravity in the classical theory of elasticity is generally neglected. The effect of gravity on the problem of propagation of waves in solids, in particular on an elastic globe, was first studied by Bromwich [13]. Ailawalia and Narah [14] depicted the effects of rotation and gravity in the generalized thermoelastic medium. Othman *et al.* [15] studied the influence of the gravitational field and rotation on the generalized thermoelastic medium using a dual-phase-lag model. Das *et al.* [16] investigated the surface waves under the influence of gravity in a non-homogeneous medium. Othman and Hilal [17] studied the rotation and gravitational field effect on two-temperature thermoelastic material with voids and temperature-dependent properties using G-N III. Abd-Alla *et al.* [18] investigated the propagation of a thermoelastic wave in a half-space of a homogeneous isotropic material subjected to the effect of gravity field. Abd-Alla *et al.* [19] studied the rotational effect on thermoelastic Stoneley,

Love and Rayleigh waves in fibre-reinforced anisotropic general viscoelastic media of higher order. The interplay of the Maxwell electromagnetic field with the motion of deformable solids is largely being undertaken by many investigators owing to the possibility of its application to geophysical problems and certain topics in optics and acoustics. Moreover, the earth is subject to its own magnetic field and the material of the earth may be electrically conducting. Thus, the magneto-elastic nature of the earth's material may affect the propagation of waves. Many authors have considered the propagation of electro-magneto-thermoelastic waves in an electrically and thermally conducting solid. A comprehensive review of the earlier contributions to the subject can be found in the study by Puri [20]. Abo-Dahab *et al.* [21] discussed the influence of thermal stress and magnetic field in thermoelastic half-space without energy dissipation. Abd-Alla and Mahmoud [22] investigated the magneto-thermoelastic problem in rotating non-homogeneous orthotropic hollow cylinder under the hyperbolic heat conduction model.

The ultra short lasers are those with the pulse duration ranging from nanoseconds to femtoseconds. The high intensity, energy flux, and ultrashort duration laser beam have been studied in situations where very large thermal gradients or an ultra-high heating rate may exist on the boundaries, this in the case of ultra-short-pulsed laser heating [23,24]. Marin [26] investigated the temporally evolutionary equation for elasticity of micropolar bodies with voids.

Marin and Stan [27] obtained the weak solutions in elasticity of dipolar bodies with stretch. Marin and Baleanu [28] studied the vibrations in thermoelasticity without energy dissipation for micropolar bodies. The microscopic two-step models that are parabolic and hyperbolic are useful for modifying the material thin films. When a metal film is heated by a laser pulse, a thermoelastic wave is generated due to thermal expansion near the surface.

The present paper aims to study the effect of gravity, magnetic field and laser pulse on the general model of the equations of generalized thermoelasticity for a homogeneous isotropic elastic half-space. The formulation is applied under four theories of generalized thermoelasticity: the coupled theory (CT), Lord-Schulman (L-S) theory, Green-Lindsay (G-L) theory as well as Green-Naghdi (G-N II) theory. By employing normal mode analysis, the analytical expressions for the temperature, displacement components and the (mechanical and Maxwell's) stresses distribution are obtained in

the physical domain. These expressions are also calculated numerically and corresponding graphs are plotted to illustrate and compare theoretical results. The effect of gravity, magnetic and laser pulse field are also studied and presented graphically to show the influence of new parameters on the phenomena.

2 Formulation of the problem and basic equations

Following the constitutive equations and field equations for a linear isotropic generalized thermoelasticity in the context of four theories, we consider a Cartesian coordinate system (x, y, z) having originated on the surface $y = 0$ and z-axis pointing vertically into the medium of a half space $(x \geq 0)$. For two-dimensional problems, we assume the dynamic displacement vector as $\overrightarrow{u} = (u, 0, w)$, and all the considered quantities are functions of the time variable t and of the coordinates x and z.

The basic governing equations of linear generalized thermoelasticity with rotation and magnetic field in the absence of heat sources are given by [22,24]:

$$\mu u_{i,jj} + (\lambda + \mu)\, u_{j,ij} - \gamma \left(1 + \theta_0 \frac{\partial}{\partial t}\right) T_{,i} + G_i = \rho \ddot{u}_i \,, \tag{1}$$

$$kT_{,ii} + k^* \dot{T}_{,ii} = \rho C_e \left(n_1 \frac{\partial}{\partial t} + \tau_0 \frac{\partial^2}{\partial t^2}\right) T + \gamma T_0 \left(n_1 \frac{\partial}{\partial t} + n_0 \tau_0 \frac{\partial^2}{\partial t^2}\right) (\nabla \cdot u) - \rho \dot{Q} \,, \tag{2}$$

$$\sigma_{ij} = \left[\lambda u_{k,k} - \left(1 + \theta_0 \frac{\partial}{\partial t}\right) T\right] \delta_{ij} + 2\mu e_{ij} \,, \qquad i, j, k = 1, 2, 3 \,, \tag{3}$$

$$e_{ij} = \frac{1}{2} \left(u_{i,j} + u_{j,i}\right) \,, \quad i, j = 1, 2, 3 \,. \tag{4}$$

The plate surface is illuminated by the laser pulse given by the heat input

$$Q = \frac{I_0 \gamma}{2\pi r^2} \exp\left(-\frac{z^2}{r^2} - \gamma x\right) f(t) \,, \tag{5}$$

where I_0 is the absorbed energy, r is the beam radius, and γ is constant.

The temporal profile can be defined as

$$f(t) = \frac{t}{t_0^2} \exp\left(-\frac{t}{t_0}\right),$$

where t_0 is the pulse rising time.

Due to the application of initial magnetic field $\mathbf{H} = H_0\mathbf{n}$, resulting in an induced magnetic field h and an induced electric field E, the simplified linear equations of electrodynamics of slowly moving medium for a homogeneous, thermally and electrically conducting elastic solid are:

$$\text{curl } \vec{\text{h}} = \vec{\text{J}} + \varepsilon_{\text{o}} \vec{\text{E}}\,, \tag{6}$$

$$\text{curl } \vec{E} = -\mu_0 \vec{h}\,, \tag{7}$$

$$\text{div } \vec{h} = 0\,, \text{div } \vec{E} = 0\,, \tag{8}$$

$$\vec{E} = -\mu_0 \left(\vec{u} \times \vec{H}\right). \tag{9}$$

The basic governing equations of a linear, homogenous thermoelastic medium under the influence of a laser pulse and the gravitational field will be in the forms:

$$\mu\nabla^2 u + (\lambda+\mu)\frac{\partial e}{\partial x} - \gamma\left(1+\theta_0\frac{\partial}{\partial t}\right)\frac{\partial T}{\partial x} + \rho g\frac{\partial w}{\partial x} - \mu_0 H_0\frac{\partial h}{\partial x} = \rho\frac{\partial^2 u}{\partial t^2}\,, \tag{10}$$

$$\mu\nabla^2 w + (\lambda+\mu)\frac{\partial e}{\partial z} - \gamma\left(1+\theta_0\frac{\partial}{\partial t}\right)\frac{\partial T}{\partial z} + \rho g\frac{\partial u}{\partial x} - \mu_0 H_0\frac{\partial h}{\partial z} = \rho\frac{\partial^2 w}{\partial t^2}\,, \tag{11}$$

$$\begin{aligned} k\nabla^2 T + k^*\frac{\partial}{\partial t}\nabla^2 T &= \rho C_e\left(n_1\frac{\partial}{\partial t} + \tau_0\frac{\partial^2}{\partial t^2}\right)T \\ &+ \gamma T_0\left(n_1\frac{\partial}{\partial t} + n_0\tau_0\frac{\partial^2}{\partial t^2}\right)(\nabla\cdot u) - \rho\frac{\partial Q}{\partial t}\,. \end{aligned} \tag{12}$$

Introducing the following dimensionless variables:

$$\{x', z'\} = \frac{\omega^*}{c_0}\{x, z\}\,,\ \vartheta_0' = \omega^*\vartheta_0,\ t' = \omega^* t,\ \tau_0' = \omega^*\tau\,, Q' = \frac{Q}{w^* T_0 C_e}\,, \tag{13}$$

$$\{u', w'\} = \frac{\rho c_0\omega^*}{\upsilon T_0}\{u, w\}\,, T' = \frac{T}{T_0},\ \delta_{ij}' = \frac{\delta_{ij}}{\upsilon T_0},\ g' = \frac{g}{c_0 w^*}\,h' = \frac{h}{H_0}\,, \tag{14}$$

where

$$\omega^* = \frac{\rho\, C_E\, c_0^2}{K}\,, \qquad \rho\, c_0^2 = \lambda + 2\mu\,.$$

Eqs. (6)–(8) will be rewritten into the non-dimensional form (with dropping primes for convenience):

$$\nabla^2 u + b_1 \frac{\partial e}{\partial x} - b_2 \left(1 + \theta_0 \frac{\partial}{\partial t}\right) \frac{\partial T}{\partial x} + b_3 \frac{\partial w}{\partial x} - R_h \frac{\partial h}{\partial x} = b_2 \frac{\partial^2 u}{\partial t^2}\,, \tag{15}$$

$$\nabla^2 w + b_1 \frac{\partial e}{\partial z} - b_2 \left(1 + \theta_0 \frac{\partial}{\partial t}\right) \frac{\partial T}{\partial z} + b_3 \frac{\partial u}{\partial x} - R_h \frac{\partial h}{\partial z} = b_2 \frac{\partial^2 w}{\partial t^2}\,, \tag{16}$$

$$\begin{aligned} \varepsilon_3 \nabla^2 T + \varepsilon_2 \frac{\partial}{\partial t} \nabla^2 T &= \varepsilon_4 \left(n_1 \frac{\partial}{\partial t} + \tau_0 \omega^* \frac{\partial^2}{\partial t^2}\right) T \\ &+ \varepsilon_1 \left(n_1 \frac{\partial}{\partial t} + n_0 \tau_0 \frac{\partial^2}{\partial t^2}\right) e - \frac{\partial Q}{\partial t}\,, \end{aligned} \tag{17}$$

where

$$\varepsilon_1 = \frac{\gamma^2 T_0}{w^* c_0^2 \rho C_e}\,,\ \varepsilon_2 = \frac{k^* w^*}{\rho c_0^2 C_e}\,,\ \varepsilon_3 = \frac{k}{\rho c_0^2 C_e}\,,\ \varepsilon_4 = \frac{1}{\omega^*},\quad b_1 = \frac{\lambda + \mu}{\mu}\,,$$

$$b_2 = \frac{\rho c_0^2}{\mu}\,,\quad b_3 = \frac{\rho g c_0^2}{\mu}\,,\quad R_h = \frac{\mu_0 H_0^2}{\mu}\,.$$

Here $\varepsilon_1, \varepsilon_2$, and ε_3 are the coupling constants.

Using the expressions relating the displacement components $u\,(x,z,t)$, and $w\,(x,z,t)$ to each of the potential functions $\psi_1\,(x,z,t)$ and $\psi_2\,(x,z,t)$ in the dimensionless forms

$$u = \frac{\partial \psi_1}{\partial x} - \frac{\partial \psi_2}{\partial z} \quad \text{and} \quad w = \frac{\partial \psi_1}{\partial z} + \frac{\partial \psi_2}{\partial x}\,. \tag{18}$$

gives

$$e = \nabla^2 \psi_1 \quad \text{and} \quad \left(\frac{\partial u}{\partial z} - \frac{\partial w}{\partial x}\right) = \nabla^2 \psi_2\,. \tag{19}$$

Using (14) and (15) into (11)–(13) yields:

$$\left[\left(1 + b_1 - R_h\right) \nabla^2 - b_2 \frac{\partial^2}{\partial t^2}\right] \psi_1 + b_3 \frac{\partial}{\partial x} \psi_2 - b_2 \left(1 + \theta_0 \frac{\partial}{\partial t}\right) T = 0\,, \tag{20}$$

$$-b_3 \frac{\partial}{\partial x} \psi_1 + \left[\nabla^2 - b_2 \frac{\partial^2}{\partial t^2}\right] \psi_2 = 0\,, \tag{21}$$

$$-\varepsilon_1\left(\frac{n_1}{\omega^*}\frac{\partial}{\partial t}+n_0\tau_0\frac{\partial^2}{\partial t^2}\right)\nabla^2\psi_1+\left(\varepsilon_3+\varepsilon_2\frac{\partial}{\partial t}\right)\nabla^2 T$$
$$-\varepsilon_4\left(n_1\frac{\partial}{\partial t}+\tau_0\omega^*\frac{\partial^2}{\partial t^2}\right)T=-\frac{\partial}{\partial t}Q\,. \tag{22}$$

The constitutive relations will be:

$$\sigma_{xx}=\frac{\partial u}{\partial x}+L\frac{\partial w}{\partial z}-\left(1+\theta_0\frac{\partial}{\partial t}\right)T\,, \tag{23}$$

$$\sigma_{yy}=L\,e-\left(1+\theta_0\frac{\partial}{\partial t}\right)T\,, \tag{24}$$

$$\sigma_{zz}=\frac{\partial w}{\partial z}+L\frac{\partial u}{\partial x}-\left(1+\theta_0\frac{\partial}{\partial t}\right)T\,, \tag{25}$$

$$\sigma_{xz}=\frac{1}{b_2}\left(\frac{\partial u}{\partial z}+\frac{\partial w}{\partial x}\right),\qquad \sigma_{xy}=\sigma_{yz}=0\,, \tag{26}$$

$$\tau_{zz}=G\left(\frac{\partial u}{\partial x}+\frac{\partial w}{\partial z}\right), \tag{27}$$

where

$$L=\frac{\lambda}{\lambda+2\mu}\,,\quad G=\frac{\mu_e H_0^2}{\lambda+2\mu}\,.$$

3 The normal mode analysis

We can decompose the solution of the physical quantities in terms of the normal mode as follows:

$$[\psi_1,\psi_2,T]\,(x,z,t)=[\psi_1^*,\psi_2^*,T^*]\,(x)\exp\left[i\left(\omega t+az\right)\right], \tag{28}$$

where $[\psi_1^*,\psi_2^*,T^*]\,(x)$ are the amplitudes of the physical quantities, ω is the angular frequency, $i=\sqrt{-1}$ and a is the wave number.

Using (28), Eqs. (20)–(22) will be:

$$\left[D^2-B_1\right]\psi_1^*+B_2D\psi_2^*-B_3\left(1+\theta_0 i\omega\right)T^*=0\,, \tag{29}$$

$$-b_3D\psi_1^*+\left[D^2-B_2\right]\psi_2^*=0\,, \tag{30}$$

$$B_5\left[D^2-a^2\right]\psi_1^*+\left[D^2-a^2\right]T^*-B_6T^*=B_7\frac{\partial}{\partial t}Q\,, \tag{31}$$

where

$$B_1 = a^2 - \frac{b_2\omega^2}{1+b_1-R_H}, \quad B_2 = \frac{b_3}{1+b_1-R_H}, \quad B_3 = \frac{b_2}{1+b_1-R_H},$$
$$B_4 = a^2 - b_2\omega^2, \quad B_5 = \frac{\varepsilon_1\omega\left(n_1 i - n_0\tau_0\omega^*\omega\right)}{(\varepsilon_3+\varepsilon_2 i\omega)},$$
$$B_6 = \frac{-\varepsilon_4\omega\left(-n_1 i + \tau_0\omega^*\omega\right)}{(\varepsilon_3+\varepsilon_2 i\omega)}, \quad \text{and } D = \frac{d}{dx}, \quad B_7 = \frac{-1}{(\varepsilon_3+\varepsilon_2 i\omega)}.$$

Eliminating ψ_1^*, ψ_2^*, and T^* from Eqs. (29)–(31) gives the differential equations:

$$\left[D^6 - B_8D^4 + B_9D^2 - B_{10}\right]\psi_1^* = B_{11}\left(1-\frac{t}{t_0}\right) \times \exp\left[-\left(\frac{z^2}{r^2}+\frac{t}{t_0}+\gamma x + i\omega t + iaz\right)\right], \tag{32}$$

$$\left[D^6 - B_8D^4 + B_9D^2 - B_{10}\right]T^* = B_{12}\left(1-\frac{t}{t_0}\right) \times \exp\left[-\left(\frac{z^2}{r^2}+\frac{t}{t_0}+\gamma x + i\omega t + iaz\right)\right], \tag{33}$$

$$\left[D^6 - B_8D^4 + B_9D^2 - B_{10}\right]\psi_2^* = B_{13}\left(1-\frac{t}{t_0}\right)\exp\left[-\left(\frac{z^2}{r^2}+\frac{t}{t_0}+\gamma x + i\omega t + iaz\right)\right], \tag{34}$$

where

$B_8 = B_1 + B_4 + B_6 + B_2b_3 - B_3B_5 - B_3B_5\vartheta_0 i + \omega + a^2,$

$B_9 = a^2B_1 + a^2B_4 + a^2B_2b_3 - a^2B_3B_5 - B_3B_5B_4 + B_1B_4 + B_6B_4 + B_1B_6 + b_3B_2B_6 + B_3B_5a^2i\omega\vartheta_0 + B_3B_4B_5i\omega\vartheta_0,$

$B_{10} = a^2B_1B_4 - a^2B_3B_5B_4 + B_1B_4B_6 - B_3B_4B_5a^2i\omega\vartheta_0,$

$B_{11} = B_3B_7\left(\gamma^2 + i\omega\vartheta_0\gamma^2 - B_4 - B_4i\omega\vartheta_0\right)\frac{I_0\gamma}{2\pi r^2t_0^2},$

$B_{12} = B_7\left[\left(\gamma^2 - B_1\right)\left(\gamma^2 - B_4\right) + \left(\gamma^2B_2b_3\right)\right]\frac{I_0\gamma}{2\pi r^2t_0^2},$

$B_{13} = -B_3B_7b_3\left(1 + i\vartheta_0\omega\right)\frac{I_0\gamma^2}{2\pi r^2t_0^2}.$

Equation (32) can be factored as

$$\left(D^2-k_1^2\right)\left(D^2-k_2^2\right)\left(D^2-k_3^2\right)\psi_1^* = B_{11}\left(1-\frac{t}{t_0}\right)\exp\left[-\left(\frac{z^2}{r^2}+\frac{t}{t_0}+\gamma x+i\omega t+iaz\right)\right], \tag{35}$$

where $k_n^2\,(n=1,2,3)$ are the roots of the characteristic equation of the homogeneous equations (32)–(34).

The general solutions of (32)–(34) bound as $x\to\infty$ are given by:

$$\psi_1(x,z,t)=\sum_{n=1}^{3}R_n\exp\left(-k_nx+i\omega t+iaz\right)+L_1B_{11}f_1\,, \tag{36}$$

$$\psi_2(x,z,t)=\sum_{n=1}^{3}H_{1n}R_n\exp\left(-k_nx+i\omega t+iaz\right)+L_1B_{13}f_1\,, \tag{37}$$

$$T(x,z,t)=\sum_{n=1}^{3}H_{2n}R_n\exp\left(-k_nx+i\omega t+iaz\right)+L_1B_{12}f_1\,. \tag{38}$$

Here

$$H_{1n}=\frac{-b_3k_n}{(k_n^2-B_4)}\,,\ n=1,2,3\,,\ H_{2n}=\frac{(k_n^2-B_1)-B_2H_{1n}k_n}{B_3}\,,\quad n=1,2,3$$

$$L_1=-\frac{1}{\gamma^6-B_8\gamma^4+B_9\gamma^2-B_{10}}\,,\ f_1=\left(1-\frac{t}{t_0}\right)\exp\left(-\frac{z^2}{r^2}-\frac{t}{t_0}-\gamma x\right),$$

where $R_n\,(n=1,2,3)$ are some undefined coefficients.

To obtain the components of the displacement vector, substituting (36) and (37) into (18) gives:

$$\begin{aligned} u(x,z,t) &= \sum_{n=1}^{3}M_{1n}R_n\exp\left(-k_nx+i\omega t+iaz\right)\\ &- \left(\gamma I_1+\frac{2zI_2}{r^2}\right)\exp\left(-\frac{z^2}{r^2}-\frac{t}{t_0}-\gamma x\right), \end{aligned} \tag{39}$$

$$\begin{aligned} w(x,z,t) &= \sum_{n=1}^{3}M_{2n}R_n\exp\left(-k_nx+i\omega t+iaz\right)\\ &+ \left(-\gamma I_2+\frac{2zI_1}{r^2}\right)\exp\left(-\frac{z^2}{r^2}-\frac{t}{t_0}-\gamma x\right), \end{aligned} \tag{40}$$

where $M_{1n} = -k_n - iaH_{1n}\,, M_{2n} = ia - k_n H_{1n}\,,\ n = 1, 2, 3.$

To get the components of the stress tensor, substitute (39), (40), and (38) into (23)–(27):

$$\begin{aligned}\sigma_{xx}(x,z,t) &= \sum_{n=1}^{3} H_{3n} R_n \exp\left(-k_n x + i\omega t + iaz\right) \\ &+ I_4 \exp\left(-\frac{z^2}{r^2} - \frac{t}{t_0} - \gamma x\right), \end{aligned} \tag{41}$$

$$\begin{aligned}\sigma_{yy}(x,z,t) &= \sum_{n=1}^{3} H_{4n} R_n \exp\left(-k_n x + i\omega t + iaz\right) \\ &+ I_5 \exp\left(-\frac{z^2}{r^2} - \frac{t}{t_0} - \gamma x\right), \end{aligned} \tag{42}$$

$$\begin{aligned}\sigma_{zz}(x,z,t) &= \sum_{n=1}^{3} H_{5n} R_n \exp\left(-k_n x + i\omega t + iaz\right) \\ &+ I_6 \exp\left(-\frac{z^2}{r^2} - \frac{t}{t_0} - \gamma x\right), \end{aligned} \tag{43}$$

$$\begin{aligned}\sigma_{xz}(x,z,t) &= \sum_{n=1}^{3} H_{6n} R_n \exp\left(-k_n x + i\omega t + iaz\right) \\ &+ I_7 \exp\left(-\frac{z^2}{r^2} - \frac{t}{t_0} - \gamma x\right), \end{aligned} \tag{44}$$

$$\begin{aligned}\tau_{xx} &= \sum_{n=1}^{3} H_{7n} \exp\left(-k_n x + i\omega t + iaz\right) \\ &+ I_8 \exp\left(-\frac{z^2}{r^2} - \frac{t}{t_0} - \gamma x\right), \end{aligned} \tag{45}$$

where

$$H_{3n} = -M_{1n}k_n + LM_{2n}ia - H_{2n} - i\omega\theta_0 H_{2n}\,,$$
$$H_{4n} = -k_n M_{1n}L + iaM_{2n}L - H_{2n} - i\omega\theta_0 H_{2n}\,,$$
$$H_{5n} = iaM_{2n} - LM_{1n}k_n - H_{2n} - i\omega\theta_0 H_{2n}\,,$$
$$H_{6n} = \tfrac{1}{b2}\left(M_{1n}ia - M_{2n}k_n\right)\,,$$
$$H_{7n} = M_{2n}Gia - M_{1n}k_n G\, I_1 = -B_{10}L_1\left(1 - \tfrac{t}{t_0}\right)\,,\ I_2 = \tfrac{B_{12}}{B_{10}}I_1\,,\ I_3 = \tfrac{B_{11}}{B_{10}}I_1\,,$$
$$I_4 = \gamma\left(\gamma I_1 - \tfrac{2z}{r^2}I_2\right) + \tfrac{2z}{r^2}\left(\gamma I_2 + \tfrac{2zI_1}{r^2}\right)L - I_3 - \tfrac{\theta_0}{t_0}I_3\,,$$
$$I_5 = E_1\gamma\left(\gamma I_1 - \tfrac{2zI_2}{r^2}\right) + L\tfrac{2z}{r^2}\left(\gamma I_2 + \tfrac{2zI_1}{r^2}\right) - I_3 - \tfrac{\theta_0}{t_0}I_3\,,$$
$$I_6 = \tfrac{2z}{r^2}\left(\gamma I_2 + \tfrac{2zI_1}{r^2}\right) + L\gamma\left(\gamma I_1 - \tfrac{2zI_3}{r^2}\right) - I_3 - \tfrac{\theta_0}{t_0}I_3\,,$$
$$I_7 = \tfrac{1}{b_2}\left[\tfrac{2z}{r^2}\left(\gamma I_1 - \tfrac{2zI_3}{r^2}\right) + \gamma\left(\gamma I_2 - \tfrac{2zI_1}{r^2}\right)\right]\,,$$
$$I_8 = G\gamma\left(\gamma I_1 - \tfrac{2zI_2}{r^2}\right) + G\tfrac{2z}{r^2}\left(\gamma I_2 + \tfrac{2zI_1}{r^2}\right)\,.$$

4 Boundary conditions

In this section, we determine the constants $R_n\,(n = 1, 2, 3)$. The boundary conditions under consideration should suppress the positive exponentials to avoid unboundedness at infinity. The coefficients R_1, R_2, R_3 are chosen such that the boundary conditions on the surface at $x = 0$ are:

I The mechanical boundary conditions

$$\sigma_{zz} + \tau_{zz} = -p_1 \exp\left(\omega t + iaz\right)\,, \quad \sigma_{xz} = 0\,. \tag{46}$$

II The thermal boundary condition on the surface of the half space

$$\frac{\partial T}{\partial x} = 0\,, \tag{47}$$

where p_1 is the magnitude of the mechanical force.

Substituting the expressions of the considered variables in the above boundary conditions, we can obtain the following equations satisfied by the parameters:

$$\sum_{n=1}^{3}(H_{5n} + H_{7n})R_n = -p\,, \tag{48}$$

$$\sum_{n=1}^{3} H_{6n}R_n = 0\,, \tag{49}$$

$$\sum_{n=1}^{3} -k_n H_{2n} R_n = 0\,. \tag{50}$$

Invoking the boundary conditions (45) and (46) at the surface $x = 0$ of the plate, we get a system of three equations (47)–(49). Solving the above system of the algebraic equations (47)–(49) by using Cramer's rule we then obtain values of the three coefficients $R_n\,(n = 1, 2, 3)$.

$$R_1 = \frac{\Delta_1}{\Delta}, \qquad R_2 = \frac{\Delta_2}{\Delta}, \qquad R_3 = \frac{\Delta_3}{\Delta}\,, \tag{51}$$

where

$$\begin{aligned}\Delta &= (H_{51} + H_{71})(-k_3 H_{62} H_{23} + k_2 H_{22} H_{62}) \\ &+ (H_{52} + H_{72})(-k_1 H_{62} H_{23} + k_3 H_{23} H_{63}) \\ &+ (H_{53} + H_{73})(-k_2 H_{61} H_{22} + k_1 H_{21} H_{62})\,,\end{aligned}$$

$$\Delta_1 = -P(-k_3 H_{62} H_{23} + k_2 H_{63} H_{22})\,,$$

$$\Delta_2 = P(-k_3 H_{61} H_{23} + k_1 H_{63} H_{21})\,,$$

$$\Delta_3 = -P(-k_2 H_{61} H_{22} + k_1 H_{62} H_{21})\,.$$

Hence, we obtain the expressions for the displacements, the temperature distribution, and the other physical quantities of the plate surface.

5 Numerical results and discussion

For numerical computations, following Dhaliwal and Singh [25] the magnesium material was chosen. All units of the parameters used in the calculation are given in SI units.

The constants of the problem are taken as:
$\lambda = 2.17 \times 10^{10}\,\mathrm{N/m^2}$, $\mu = 3.278 \times 10^{10}\,\mathrm{N/m^2}$, $K = 1.7 \times 10^2\,\mathrm{W/mK}$,
$\rho = 1.74 \times 10^3\,\mathrm{kg/m^{3,}}$, $C_e = 1.04 \times 10^3\,\mathrm{J/kgK}$, $\omega^* = 3.58 \times 10^{11}/\mathrm{s}$,
$\mu_0 = 4 \times \pi \times 10^{-3}$, $T_0 = 298\,\mathrm{K}$.
The laser pulse parameters are:
$I_0 = 10^2\ \mathrm{J/m^2}$, $r = 0.2$, $\gamma = 25/\mathrm{m}$, $t_0 = 10$.
The comparisons were carried out for:
$p_1 = 0.25\,\mathrm{N/m^2}$, $k^* = 100\,\mathrm{W/mK}$, $a = 0.5$, $\omega = 2.9\,\mathrm{rad/s}$, $z = 2\,\mathrm{m}$,
$t = 0.9\,\mathrm{s}$, $g = 9.8\,\mathrm{m/s^2}$, and $x = 0$–3.5 m.

The obtained 2D curves describe the change of behavior of the values of

the real part of the temperature distribution T, components of displacement u and w, normal stresses σ_{xx}, σ_{zz} and tangential stress σ_{xz} with distance x, for CT, L-S, G-L, and G-N theories have been shown in generalized thermoelasticity medium with constants $H_0 = 9 \times 10^5$, $g = 9.8$, $t = 0.9$, on the other hand with different values of gravity, laser pulse and magnetic field. These distributions are shown graphically in Figs. 1–32 for time $t = 0.9$ with respect to a wide range of $0 \leq x \leq 3.5$. These figures represent the solution obtained using the CT theory: $n_0 = 0\,, n_1 = 1\,, \tau_0 = 0\,, \vartheta_0 = 0$, L-S theory: $n_0 = 1\,, n_1 = 1\,, \tau_0 = 0.2\,, \vartheta_0 = 0$, G-L theory: $n_0 = 0\,, n_1 = 1\,, \tau_0 = 0.2\,, \vartheta_0 = 0.3$, and G-N theory: $n_0 = 0\,, n_1 = 1\,, \tau_0 = 1\,, \vartheta_0 = 0$. We notice that the results for the temperature, displacement, and stress distributions when the relaxation time is included in the heat equation are distinctly different from those when the relaxation time is not included in the heat equation, because the thermal waves in Fourier's theory travel with an infinite speed of propagation as opposed to the finite speed in the non-Fourier case. This demonstrates clearly the difference between the coupled and the generalized theories of thermoelasticity. Also, these distributions are shown graphically in Figs. 9–16 with different values of gravity: $g = 0$, 5, 7, and 9.8. Also, these distributions are shown graphically in Figs. 17–24 with different values of laser pulse: $t = 0$, 0.3, 0.6,, and 0.9, and in Figs. 25–32 with different values of magnetic field: $H_0 = 0$, 2×10^5, 3×10^5, and 5×10^5. The distributions of all physical quantities converge to zero as the distance x tends to infinity.

Figure 1 shows the distribution of displacement component u with respect to x-axis. The effects of parameters of the theories on the curves are the strongest for the G-N theory, after that L-S after that G-L, and the smallest effects concern the theory CT.

Figure 2 displays the distribution of displacement component w with respect to x-axis. We note the difference in effects according to different theories where the effects are strong in the theory of G-N while in other theories are weak.

Figures 3, 4, and 7 illustrate the distribution of normal stress σ_{xx}, σ_{zz} and $\tau_{zz} + \sigma_{zz}$ with respect to x-axis. The effects of parameters of the theories on the curves are the strongest for the G-N theory, while in other theories are weak.

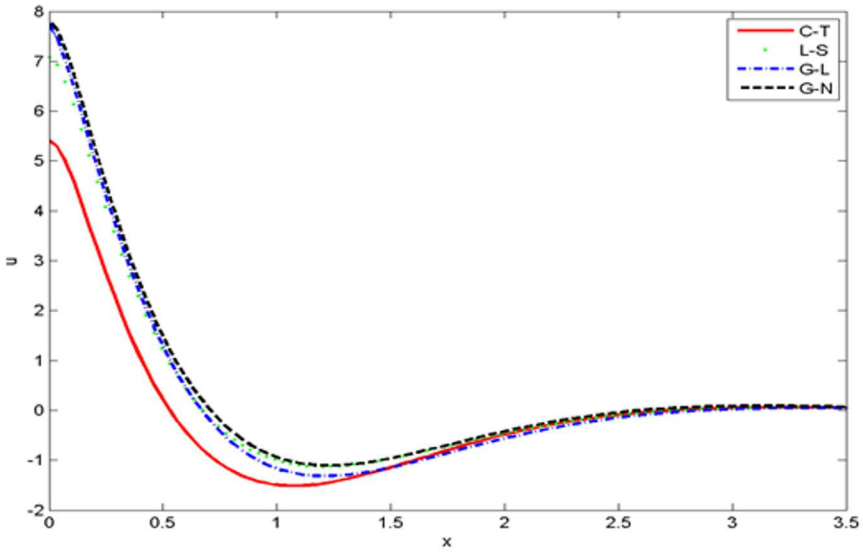

Figure 1: Displacement u distribution versus x calculated with the help of four theories.

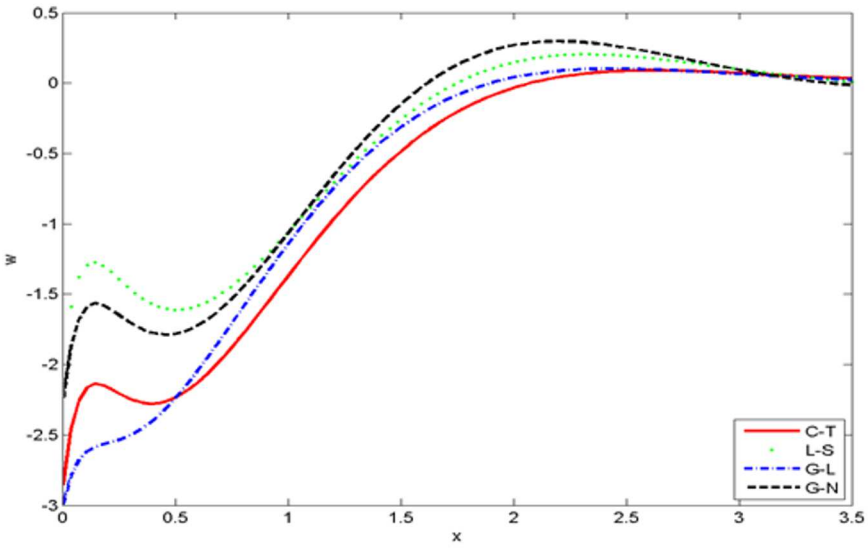

Figure 2: Displacement w distribution versus x calculated with the help of four theories.

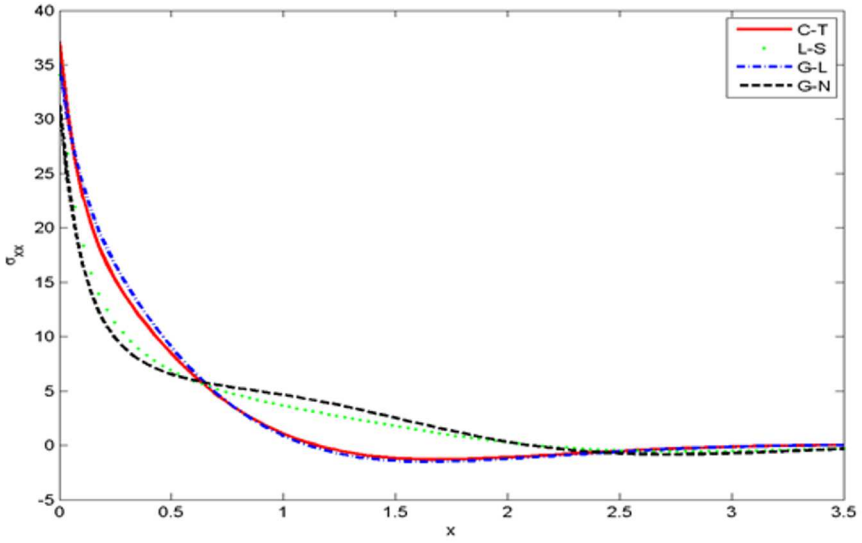

Figure 3: Stress distribution σ_{xx} versus x calculated with the help of four theories.

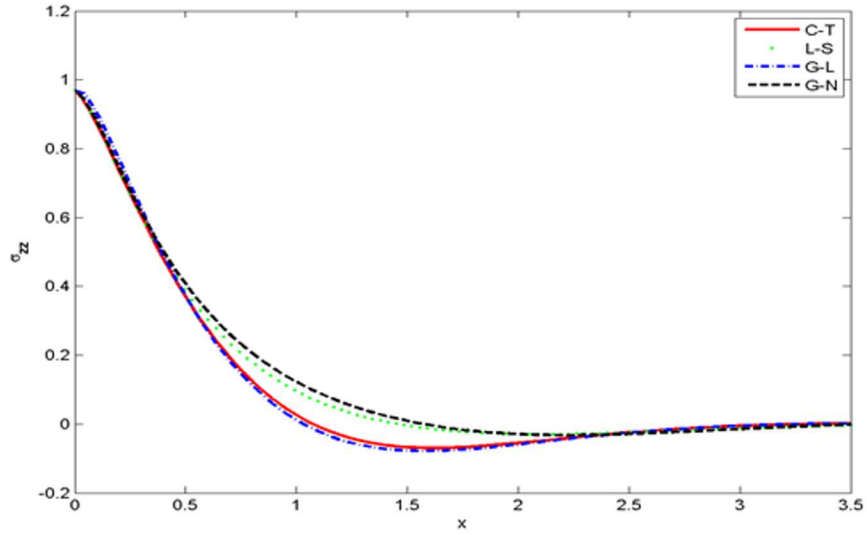

Figure 4: Stress distribution σ_{zz} versus x calculated with the help of four theories.

Figure 5 shows the distribution of tangential stress σ_{xz} with respect to x-axis. It is clear that all curves always begin from zero for the four theories to satisfy the boundary condition at $x = 0$, We note the difference in effects according to different theories, where the effects are strong in the theory of G-N, while in other theories are weak.

Figure 6 illustrates the distribution of normal stress τ_{zz} with respect x-axis. The effects of parameters of the theories on the curves are the strongest for the CT theory, while in other theories are weak.

Figure 8 displays the distribution of temperature T with respect to x-axis. We note the difference in effects according to different theories where the effects are strong in the theory of CT while in other theories are weak.

Figures 9 and 10 show the distribution of displacement components u, w with respect to x-axis for different values of gravity field g. It is observed that the displacement component u decreases with the increasing gravity field in the interval $[0, 3]$ except at $g = 0$ in the interval $[1.8, 3]$, while it tends to zero in the interval [3, 3.5]. The displacement component w decreases with the increasing gravity field in the interval [0,3] and it tends to zero in the interval [3, 3.5].

Figures 11 and 12 show the distribution of normal stress components σ_{xx}, σ_{zz} with respect to x-axis for different values of gravity field g. It is observed that the normal stress component σ_{xx} decreases with the increasing gravity field in the interval [0, 0.5], while it increases with the increasing gravity field in the interval [0.5, 3]. It tends to zero in the interval $[3, 3.5]$. The normal stress component σ_{zz} increases with the increasing gravity field in the interval [0,3], while it approaches zero in the interval [3, 3.5].

Figure 13 describes the distribution of tangential stress component σ_{xz} with respect to x-axis for different values of gravity field g. It is observed that the tangential stress component increases with the increasing gravity field in the interval [0, 3.2], while it tends to zero in the interval [3.2, 3.5].

Figures 14 and 15 illustrate the distribution of magnetic stress component τ_{zz} and total magnetic and normal stress $\tau_{zz} + \sigma_{zz}$ with respect to x-axis for different values of gravity field g. An increase of these quantities is observed with the increasing gravity field in the interval [0,3], while tend to zero in the interval [3, 3.5].

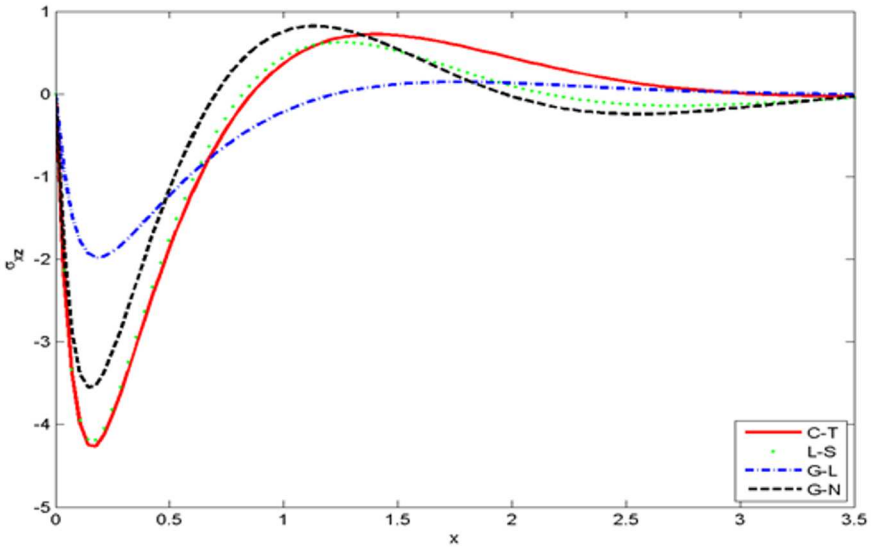

Figure 5: Stress distribution σ_{xz} versus x calculated with the help of four theories.

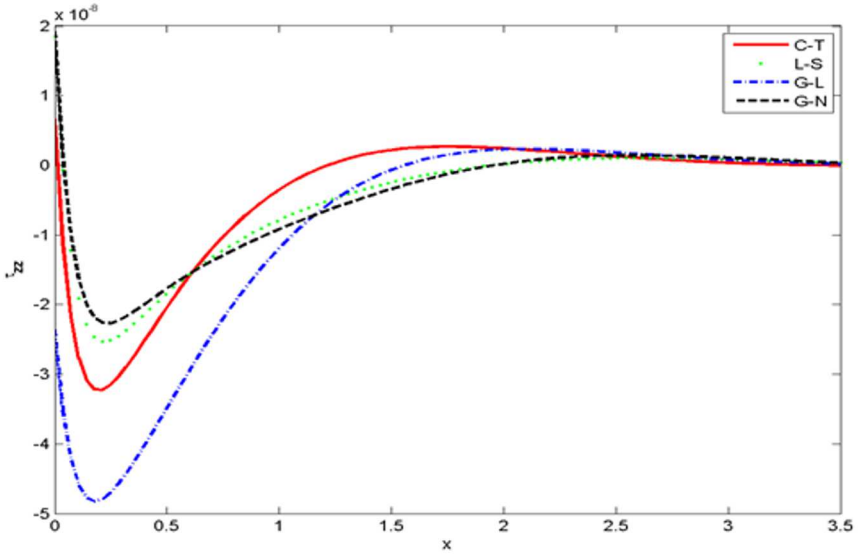

Figure 6: Stress distribution τ_{zz} versus x calculated with the help of four theories.

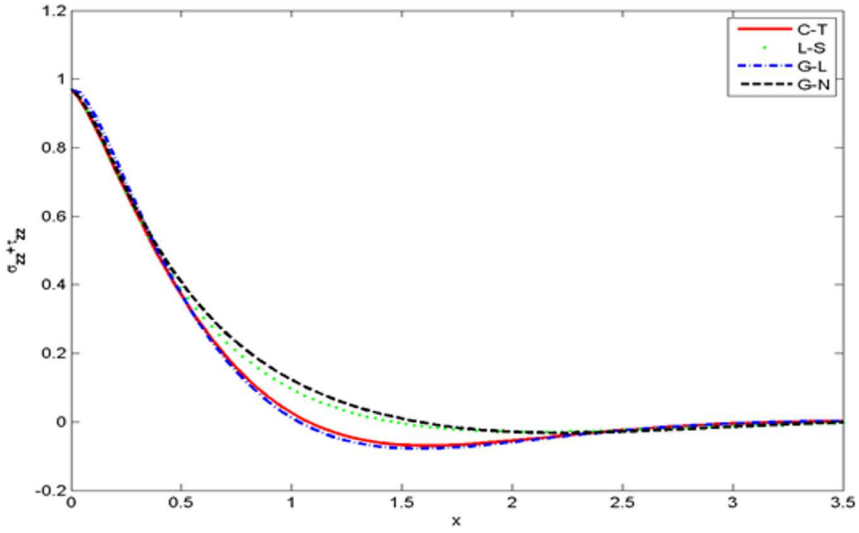

Figure 7: Stress distribution $\tau_{zz} + \sigma_{zz}$ versus x calculated with the help of four theories.

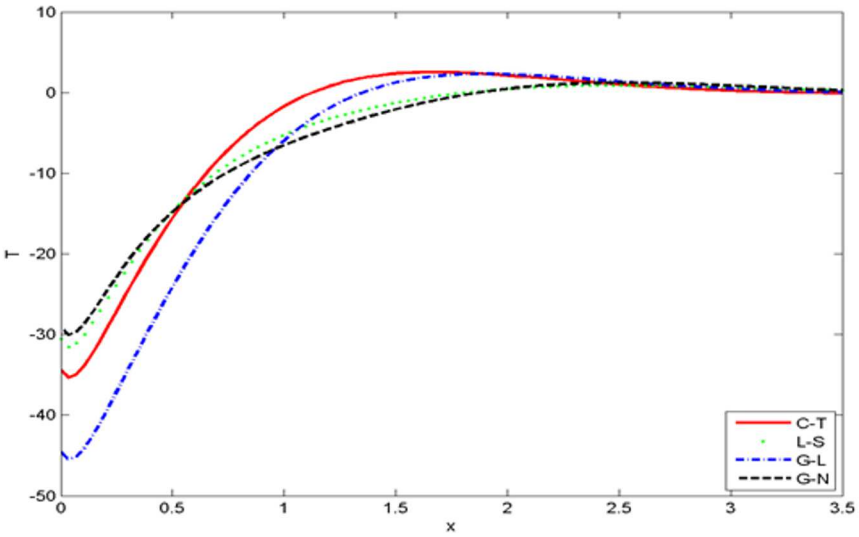

Figure 8: Temperature distribution T versus x calculated with the help of four theories.

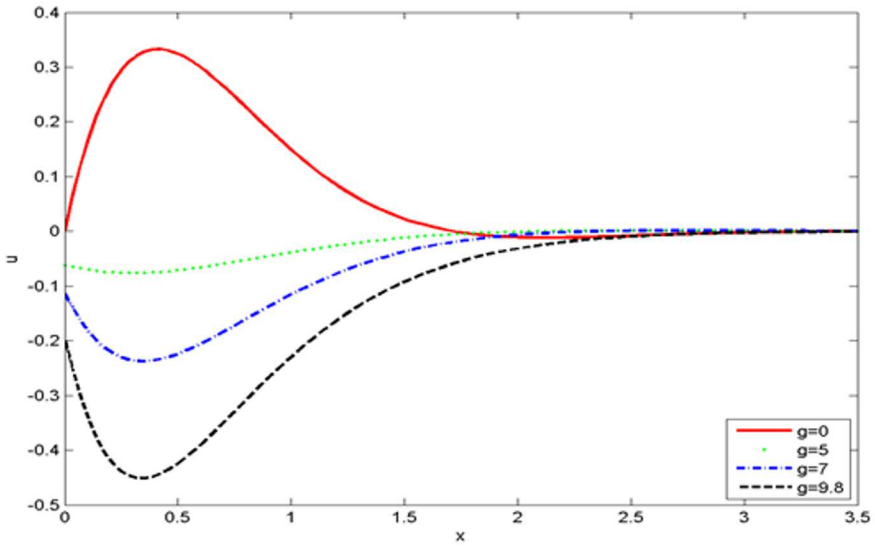

Figure 9: Displacement distribution u versus x under the effect of gravity force.

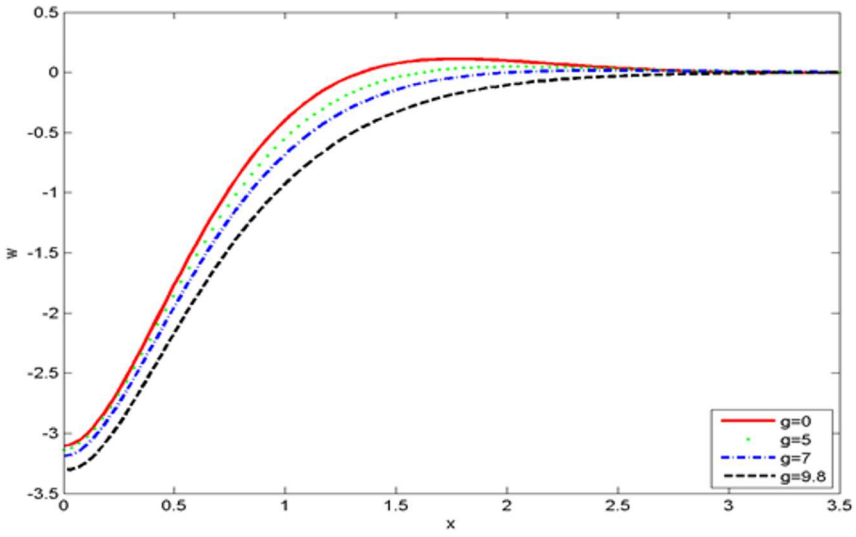

Figure 10: Displacement distribution w versus x under the effect of gravity force.

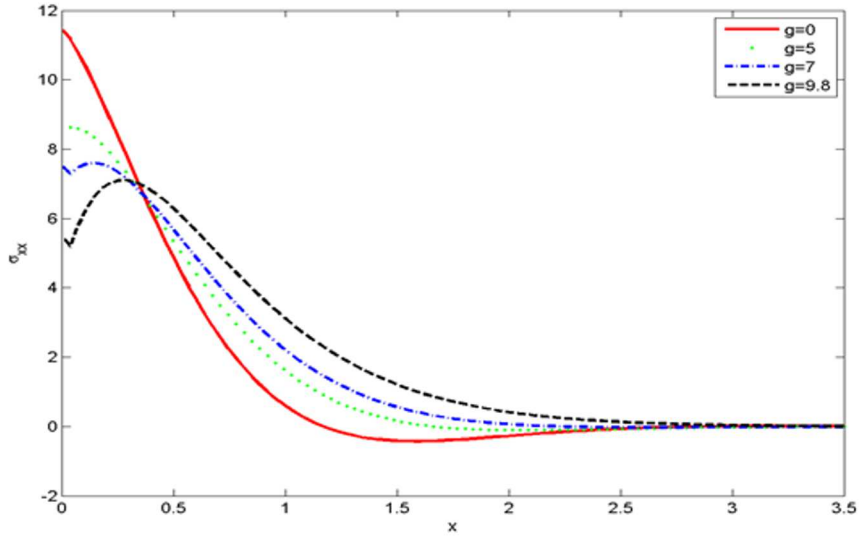

Figure 11: Stress distribution σ_{xx} versus x under the effect of gravity force.

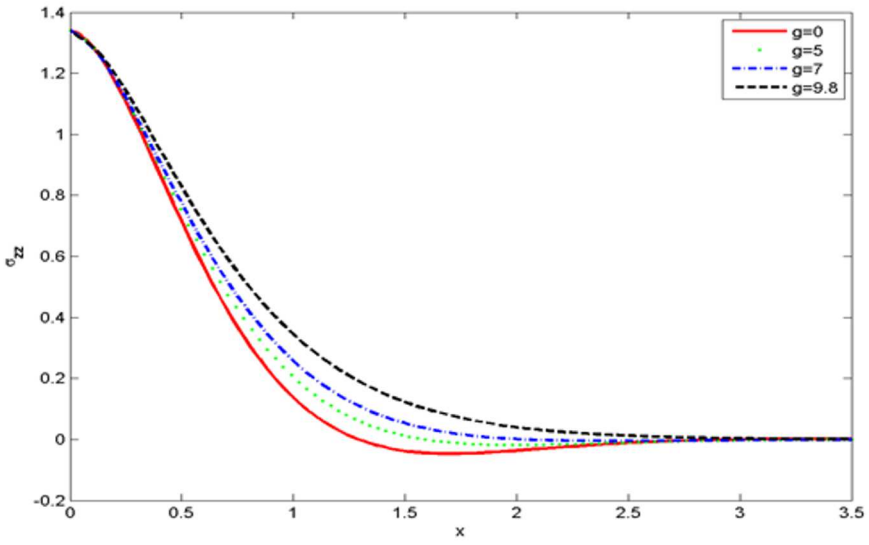

Figure 12: Stress distribution σ_{zz} versus x under the effect of gravity force.

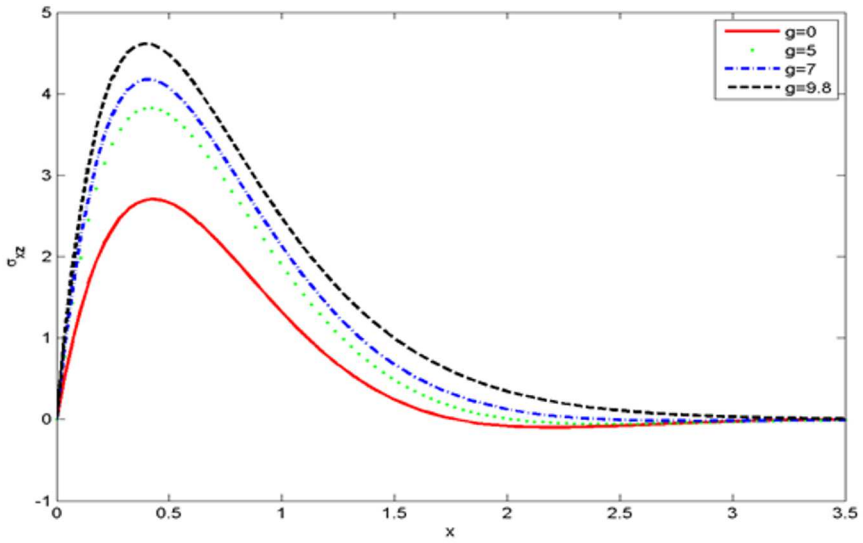

Figure 13: Stress distribution σ_{xz} versus x under the effect of gravity force.

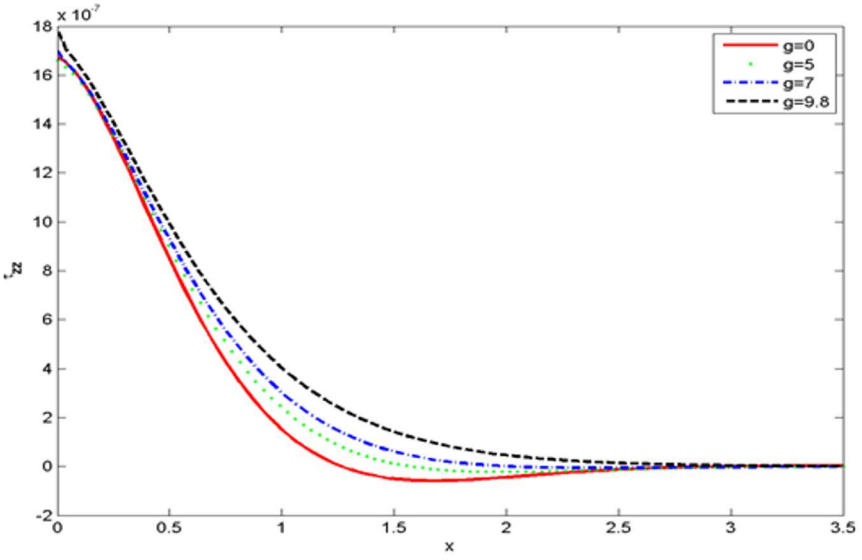

Figure 14: Stress distribution τ_{zz} versus x under the effect of gravity force.

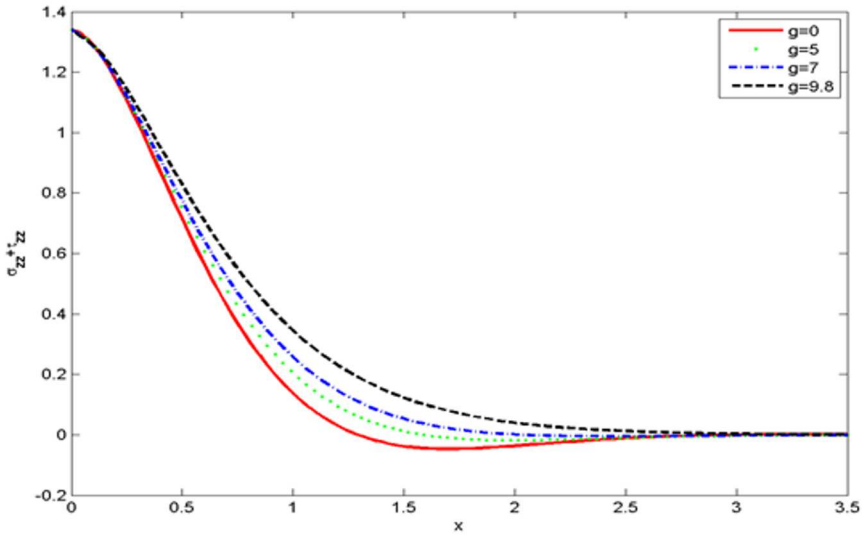

Figure 15: Stress distribution $\tau_{zz} + \sigma_{zz}$ versus x under the effect of gravity force.

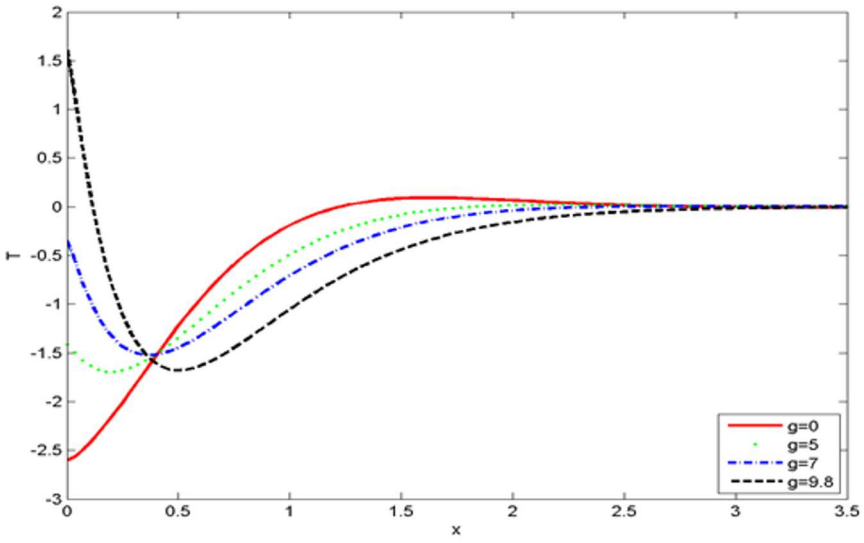

Figure 16: Temperature distribution T versus x under the effect of gravity force.

Figure 16 shows the distribution of temperature T with respect to x-axis for different values of gravity field g. The temperature has an oscillatory behavior for a thermoelastic medium in the interval $[0, 3]$. It is observed that the temperature increases with the increasing gravity field in the interval [0, 0.5], while it decreases with the increasing gravity field in the interval [0.5, 3]; and it tends to zero in the interval [3, 3.5].

Figures 17 and 18 present the distribution of displacement components u, w with respect to x-axis for different values of laser pulse t. It is observed that the displacement component u increases with the increasing laser pulse in the interval [0,3], while it decreases with the increasing the laser pulse in the interval [0.3, 1.4], and tends to zero in the interval [1.4, 3.5]. The displacement component w increases with the increasing laser pulse in the interval [0, 1.1], while it decreases with the increasing the laser pulse in the interval [1.1, 2.3], and approaches zero in the interval [2.3, 3.5].

Figures 19 and 20 show the distribution of normal stress components σ_{xx}, σ_{zz} with respect to x-axis for different values of laser pulse t. The normal stress components have an oscillatory behaviour for a thermoelastic medium in the interval [0, 2.5]. It is observed that the normal stress component σ_{xx} increases with the increasing laser pulse in the interval [0, 0.8], while it decreases with the increasing laser pulse in the interval [0.8, 2], and tends to zero in the interval [2, 3.5]. The normal stress component σ_{zz} increases with the increasing laser pulse in the interval [0,3], while it decreases with the increasing laser pulse in the interval [0.3, 1.5], as well it increases with the increasing laser pulse in the interval [1.5, 2.5] and it approaches zero in the interval [2.5, 3.5].

Figure 21 illustrates the distribution of tangential stress component σ_{xz} with respect to x-axis for different values of laser pulse t. The tangential stress has an oscillatory behaviour for a thermoelastic medium in the interval [0, 2.5]. It is observed that the tangential stress component decreases with the increasing laser pulse in the interval [0, 1.4], while it increases with the increasing laser pulse in the interval [1.4, 2.5], and it tends to zero in the interval [2.2, 3.5].

Figures 22, 23 show the distribution of magnetic stress component τ_{zz} and total magnetic and normal stress $\tau_{zz} + \sigma_{zz}$ with respect to x-axis for different values of laser pulse t. The magnetic stress component and total magnetic and normal stress have an oscillatory behaviour for a thermoelastic medium in the interval [0, 2.5]. It is observed that the magnetic stress component decreases with the increasing laser pulse in the interval [0,1],

while it increases with the increasing laser pulse in the interval [1, 2.2], and it tends to zero in the interval [2.2,3.5]. The total magnetic and normal stress increase with the increasing laser pulse in the interval [0, 0.4], while they decrease with the increasing laser pulse in the interval [0.4, 1.6], they increase with the increasing laser pulse in the interval [1.6, 2.5] and tend to zero in the interval [2.5, 3.5].

Figure 24 exhibits the distribution of temperature T with respect to x-axis for different values of time t. The temperature has an oscillatory behaviour for a thermoelastic medium in the interval [0,2]. It is observed that the temperature decreases with the increasing laser pulse in the interval [0, 0.8], while it increases with the increasing laser pulse in the interval [0.8, 2], and it approaches zero in the interval [2, 3.5].

Figure 25 shows the distribution of displacement component u with respect to x-axis for different values of magnetic field H_0. It is observed that the displacement component u increases with the increasing magnetic field in the interval [0, 0.1], while it decreases with the increasing magnetic field in the interval [0.1, 1.4], increases with the increasing magnetic field in the interval [1.4, 2.5], and it tends to zero in the interval [2.5, 3.5].

Figure 26 illustrates the distribution of displacement component w with respect to x-axis for different values of magnetic field H_0. It is observed that the displacement component increases with the increasing magnetic field in the interval [0,1.2], while it tends to zero in the interval [1.2, 3.5].

Figures 27 and 28 show the distribution of normal stress components σ_{xx}, σ_{zz} with respect to x-axis for different values of magnetic field H_0. The normal stress components have an oscillatory behaviour for a thermoelastic medium in the interval [0,2]. It is observed that the normal stress component σ_{xx} increases with the increasing time in the interval [0, 0.8], while it decreases with the increasing magnetic field in the interval [0.8, 1.7], and it tends to zero in the interval [1.7, 3.5]. The normal stress component σ_{zz} decreases with the increasing magnetic field in the interval [0, 1.5], while it increases with the increasing magnetic field in the interval [1.5, 2] and it tends to zero in the interval [2, 3.5].

Figure 29 exhibits the distribution of tangential stress component σ_{xz} with respect to x-axis for different values of magnetic field H_0. The tangential stress has an oscillatory behaviour for a thermoelastic medium in the in the interval [0, 2.2]. It is observed that the tangential stress component decreases with the increasing magnetic field in the interval [0,1], while it increases with the increasing magnetic field in the interval [1, 2.2], and it

approaches zero in the interval [2.2, 3.5].

Figures 30 and 31 present the distribution of magnetic stress component τ_{zz} and total magnetic and normal stress $\tau_{zz} + \sigma_{zz}$ with respect to x-axis for different values of magnetic field H_0. The magnetic stress component and total magnetic and normal stress have an oscillatory behaviour for a thermoelastic medium in the interval [0, 2.5]. It is observed that the magnetic stress component decreases with the increasing magnetic field in the interval [0,1], while it increases with the increasing magnetic field in the interval [1, 2.2], and it tends to zero in the interval [2.2, 3.5]. The total magnetic and normal stress decrease with the increasing magnetic field in the interval [0, 1.4], while they increase with the increasing magnetic field in the interval [1.4, 2.5], and tend to zero in the interval [2.5, 3.5].

Figure 32 shows the distribution of temperature T with respect to x-axis for different values of magnetic field H_0. The temperature has an oscillatory behaviour for a thermoelastic medium in the interval [0,2]. It is observed that the temperature decreases with the increasing magnetic field in the interval [0, 0.8], while it increases with the increasing magnetic field in the interval [0.8, 2], and it approaches zero in the interval [2, 3.5].

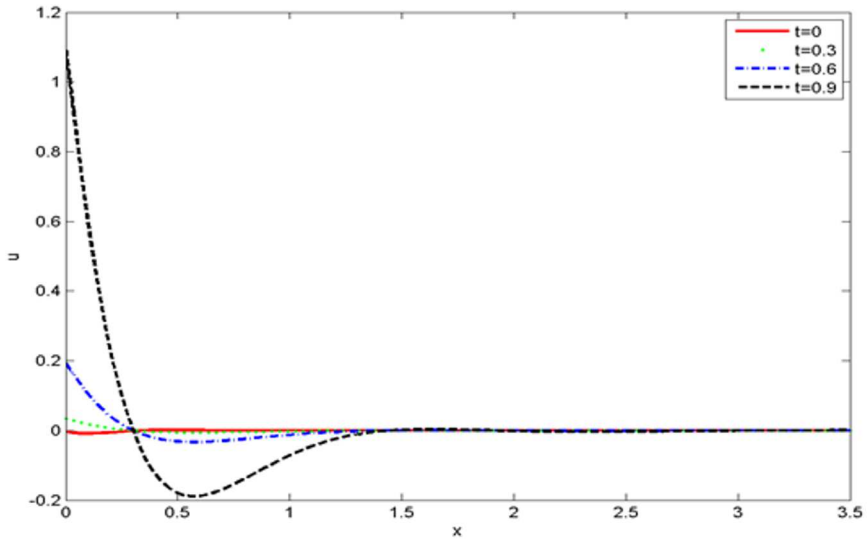

Figure 17: Displacement distribution u versus x under the effect of laser pulse.

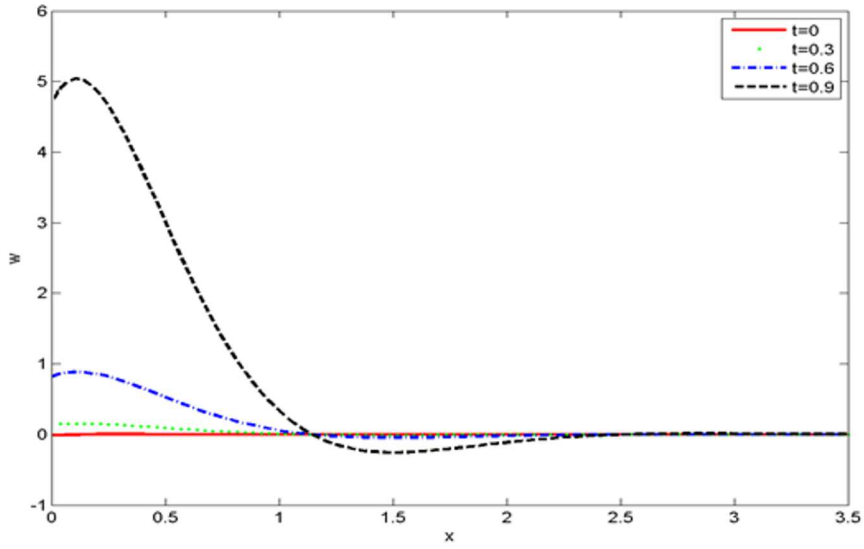

Figure 18: Displacement distribution w versus x under the effect of laser pulse.

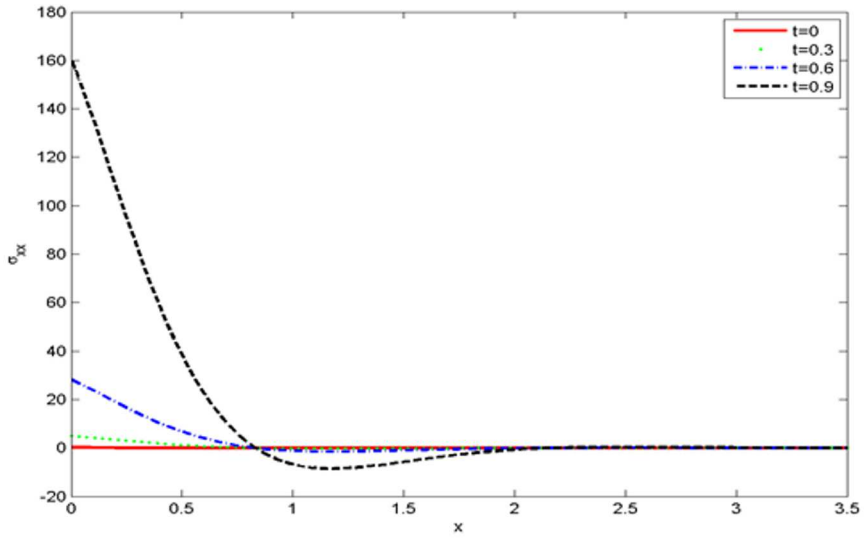

Figure 19: Stress distribution σ_{xx} versus x under the effect of laser pulse.

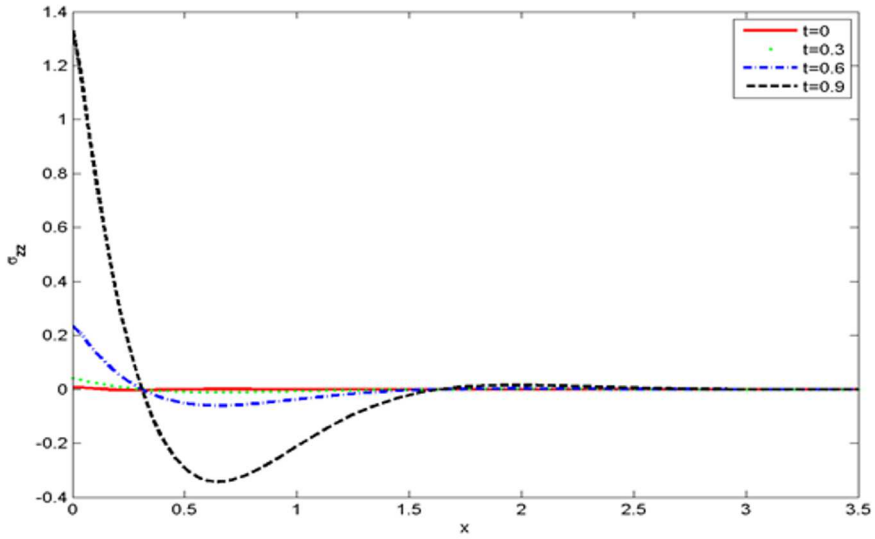

Figure 20: Stress distribution σ_{zz} versus x under the effect of laser pulse.

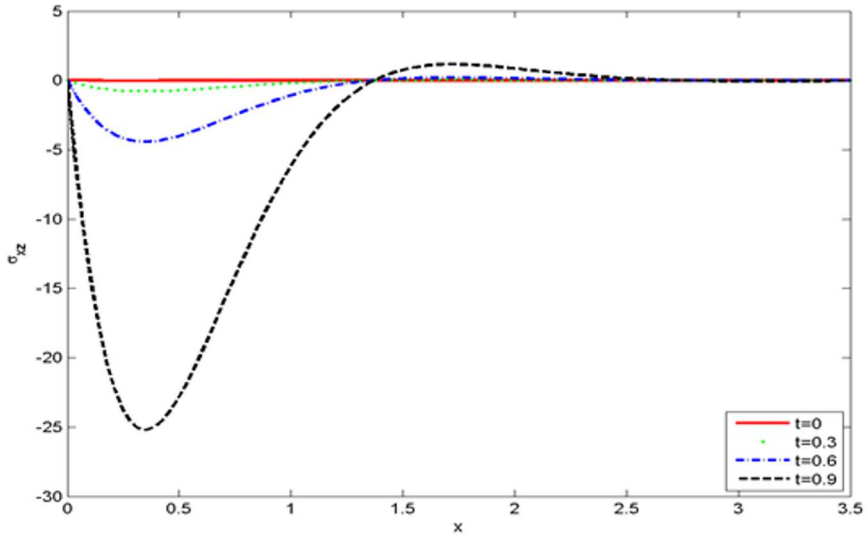

Figure 21: Stress distribution σ_{xz} versus x under the effect of laser pulse.

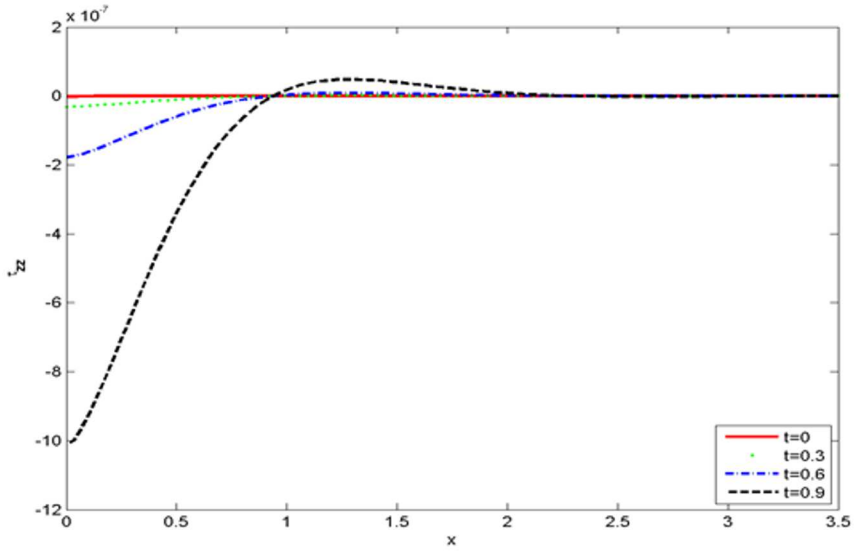

Figure 22: Stress distribution τ_{zz} versus x under the effect of laser pulse.

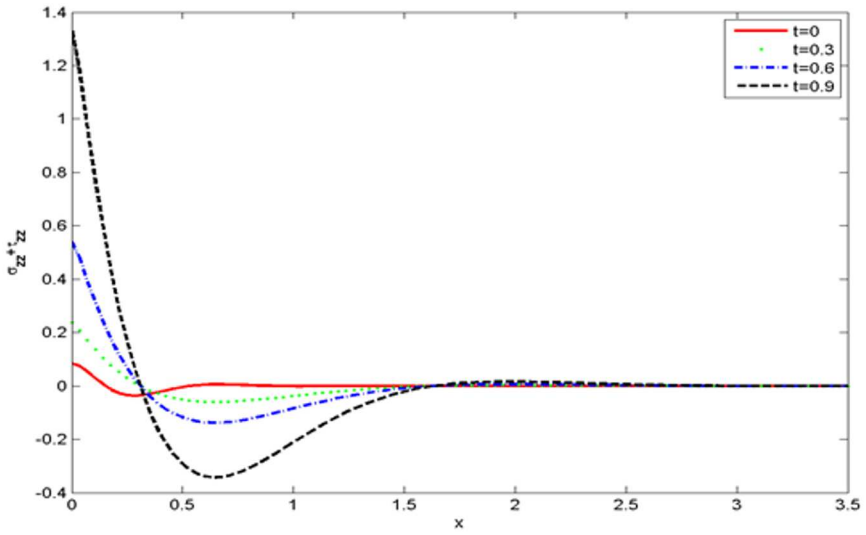

Figure 23: Stress distribution $\tau_{zz} + \sigma_{zz}$ versus x under the effect of laser pulse.

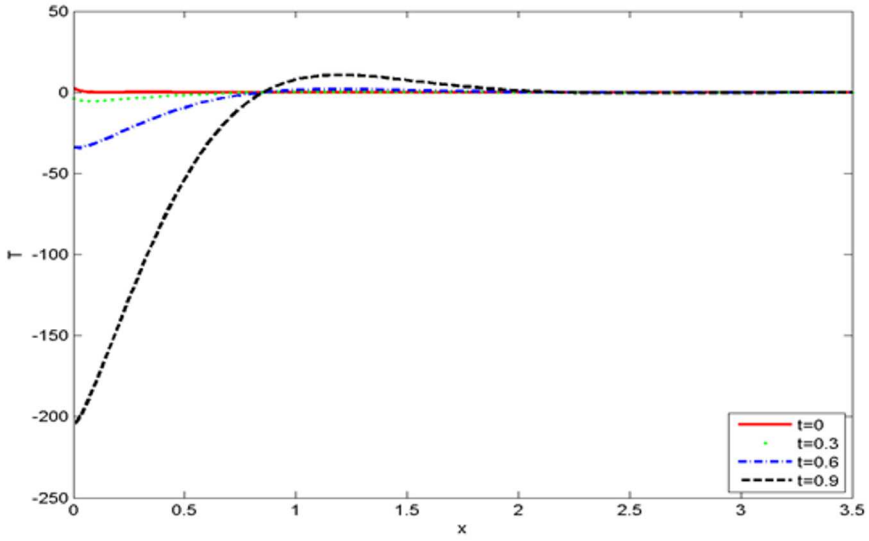

Figure 24: Temperature distribution T versus x under the effect of laser pulse.

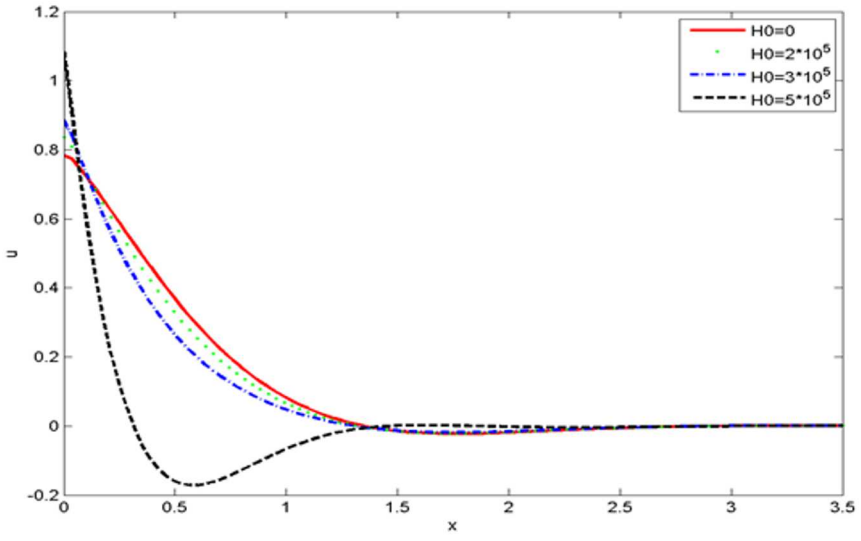

Figure 25: Displacement distribution u versus x under the effect of magnetic field.

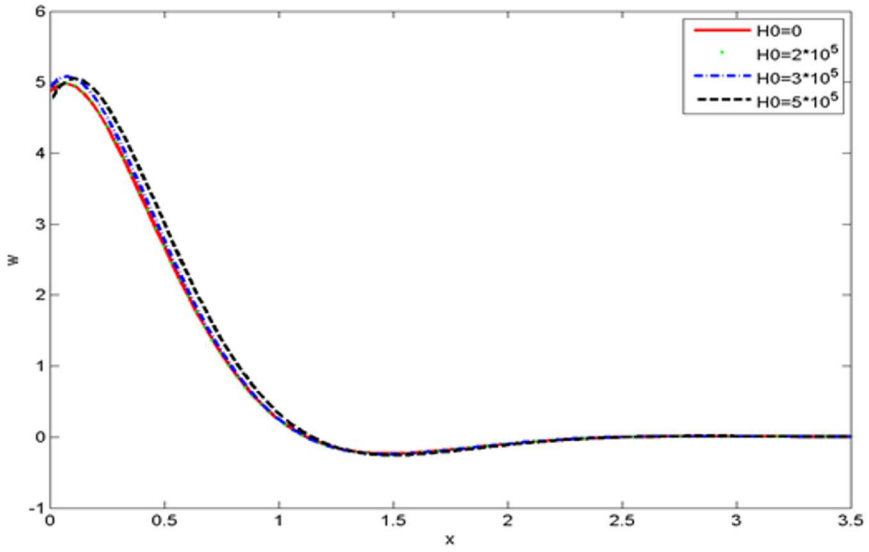

Figure 26: Displacement distribution w versus x under the effect of magnetic field.

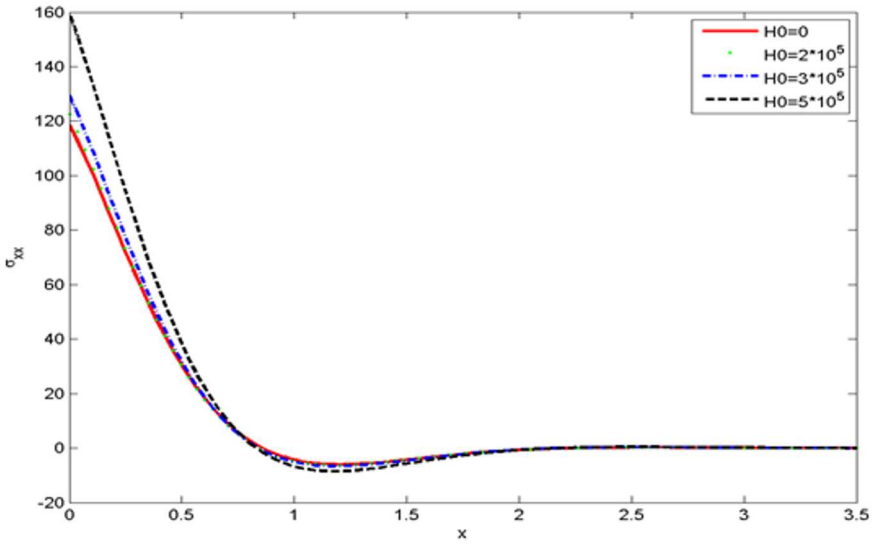

Figure 27: Stress distribution σ_{xx} versus x under the effect of magnetic field.

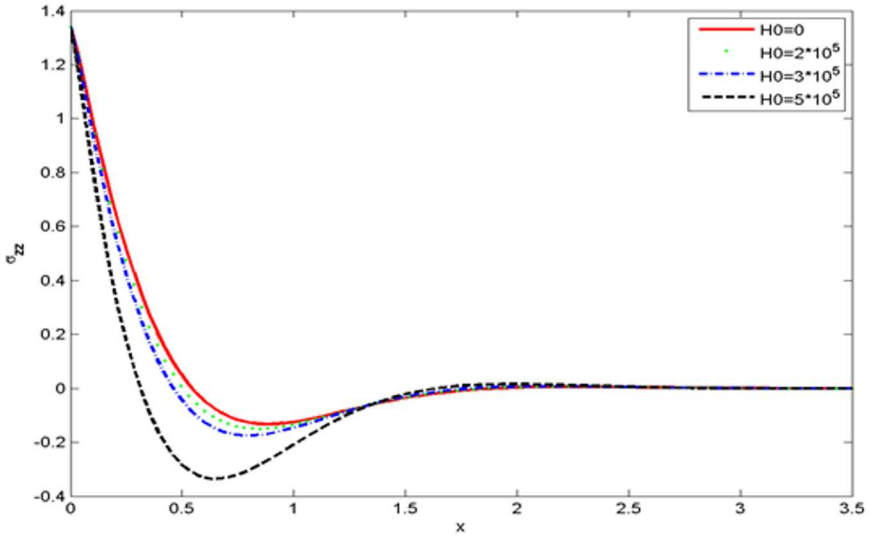

Figure 28: Stress distribution σ_{zz} versus x under the effect of magnetic field.

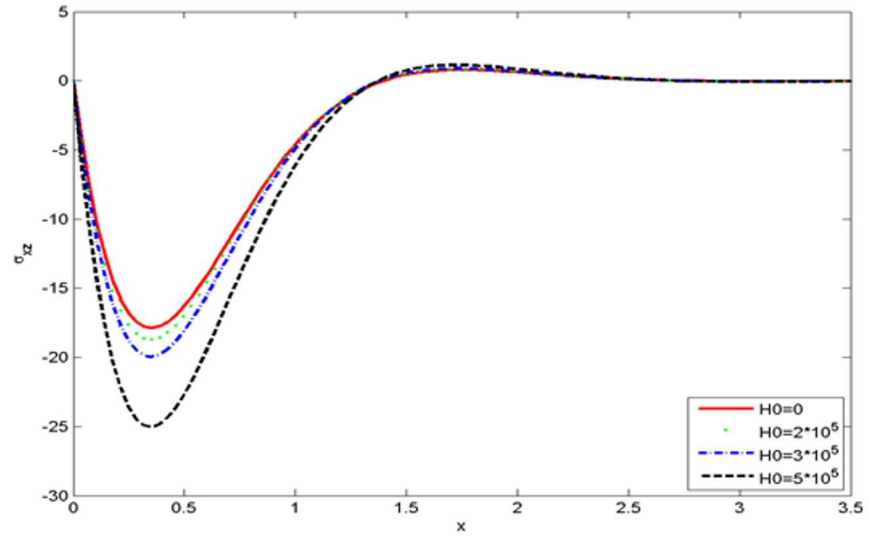

Figure 29: Stress distribution σ_{xz} versus x under the effect of magnetic field.

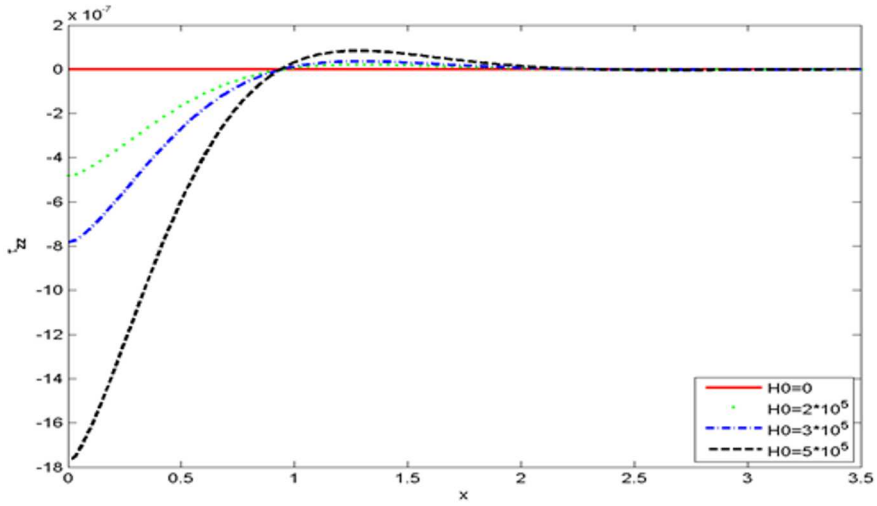

Figure 30: Stress distribution τ_{zz} versus x under the effect of magnetic field.

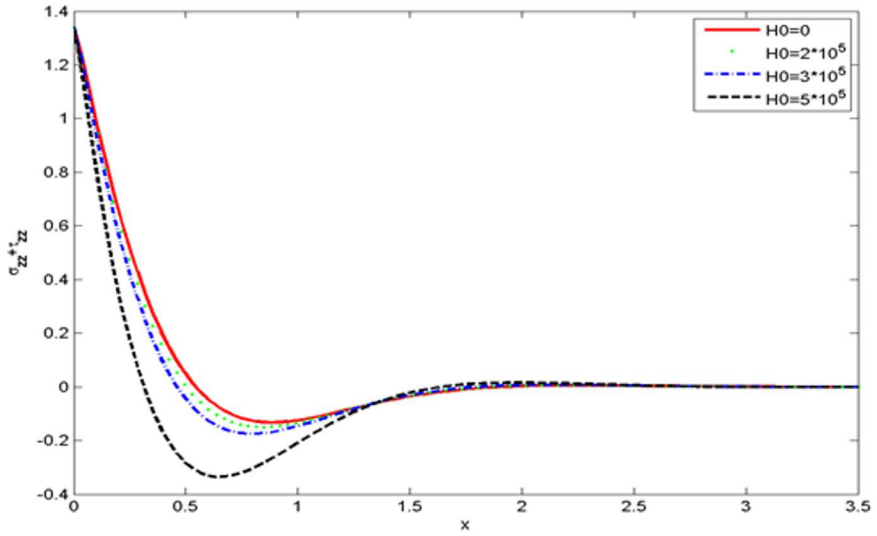

Figure 31: Displacement distribution $\tau_{zz}+\sigma_{zz}$ versus x under the effect of magnetic field.

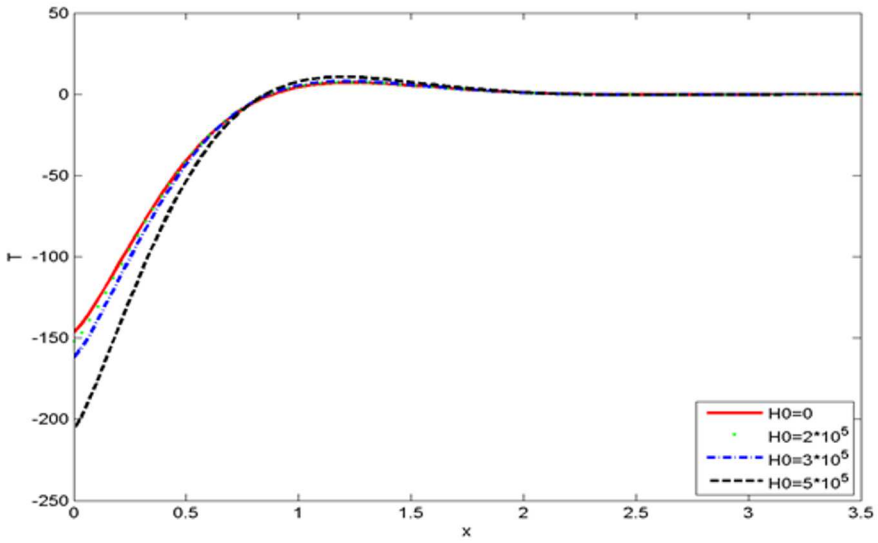

Figure 32: Temperature distribution T versus x under the effect of magnetic field.

6 Conclusions

The results of the present work can be summarized as:

1. The method which is presented in the paper is applicable to a wide range of problems in thermodynamics and thermoelasticity.

2. The presence of a magnetic field plays a significant role in all the physical quantities. The temperature, displacement components, and stress components decrease or increase. Therefore, the presence of gravity field, laser pulse, and a magnetic field in the current model is of significance.

3. The results are graphically described for the medium of crystal. The present theoretical results may provide interesting information for experimental scientists/researchers /seismologists working on this subject.

4. All the physical quantities satisfy the boundary conditions.

5. The values of all physical quantities converge to zero with the increasing distance x, and all functions are continuous.

6. The gravity field, magnetic field and time as a physical operator have a significant role in the considered physical quantities.

7. The result provides a motivation to investigate conducting magneto-thermoelectric materials as a new class of applicable magneto-thermoelectric solids. The results presented in this paper should prove useful for researchers in material science, designers of new materials, physicists as well as for those working on the development of magneto-thermo-elasticity and in practical situations as in geophysics, optics, acoustics, geomagnetic and oil prospecting, etc.

Received 8 April 2018

References

[1] Abo-Dahab S.M., Abd-Alla A.M., Kilicman A.: *Propagation of p- and T-waves in solid-liquid of thermoelastic media subjected to initial stress and magnetic field in the context of CT-theory*. J. Mech. Sci. Technol. **29**(2015), 579–591.

[2] Abo-Dahab S.M., Abd-Alla A.M.: *Effects of voids and rotation on plane waves in generalized thermoelasticity*. J. Mech. Sci. Technol. **27**(2014), 3607–3614.

[3] Abd-Alla A.M., Abo-Dahab S.M., Al-Thamali T.A.: *Propagation of Rayleigh waves in a rotating orthotropic material elastic half-space under initial stress and gravity*. J. Mech. Sci. Technol. **26**(2012), 2815–2823.

[4] Abd-Alla A.M., Mahmoud S.R.: *Analytical solution of wave propagation in a non-homogeneous orthotropic rotating elastic media*. J. Mech. Sci. Technol. **26**(2012), 917–926.

[5] Abo-Dahab S.M., Abd-Alla A.M., ELSirafy Ibrahim H.: *Effect of gravity field, initial stress and rotation on the S-waves propagation in a non-homogeneous anisotropic medium with magnetic field*. J. Mech. Sci. Technol. **28**(2014), 3003–3011.

[6] Abd-Alla A.M., Abo-Dahab S.M., Bayones F.S.: *Propagation of Rayleigh waves in magneto-thermo-elastic half-space of a homogeneous orthotropic material under the effect of rotation, initial stress and gravity field*. J. Vib. Control **19**(2013), 1395–1420.

[7] Abd-Alla A.M., Mahmoud S.R.: *On the problem of radial vibrations in non-homogeneity isotropic cylinder under influence of initial stress and magnetic field*. J. Vib. Control **19**(2013), 1283–1293.

[8] Biot M.A.: *Thermoelasticity and irreversible thermodynamics*. J. Appl. Phys. **27**(1956), 240–253.

[9] Lord H.W., Shulman Y.A.: *Generalized dynamical theory of thennoelasticity*. J. Mech. Phys. Solids **15**(1967), 299–306.

[10] Green A.E., Lindsay K.A.: *Thermoelasticity*. J. Elasticity **2**(1972), 1–7.

[11] Green A.E., Naghdi P.M.: *Thermoelasticity without energy dissipation*. J. Elasticity **31**(1993), 189–208.

[12] Green A.E., Naghdi P.M.: *On undamped heat waves in an elastic solid*. J. Therm. Stresses **15**(1992), 253–264.

[13] Bromwich T.J.: *On the influence of gravity on elastic waves and in particular on the vibrations of an elastic globe*. Proc. London Math. Soc. **30**(1898), 98–120.

[14] Ailawalia P., Narah N.S.: *Effect of rotation in generalized thermoelastic solid under the influence of gravity with an overlying infinite thermoelastic fluid*. Appl. Math. Mech. **30**(2009), 1505–1518.

[15] Othman M.I.A., Hasona W.M., Eraki E.E.M.: *Influence of gravity field and rotation on a generalized thermoelastic medium using a dual-phase-lag model*. J. Thermoelasticity **1**(2013), 12–22.

[16] Das S.C., Acharya D.P., Sengupta P.R.: *Surface waves in an inhomogeneous elastic medium under the influence of gravity*. Rev. Roumaine Sci. Techniq. **37**(1992), 539–551.

[17] Othmanand M.I.A., Hilal M.I.M.: *Rotation and gravitational field effect on two-temperature thermoelastic material with voids and temperature dependent properties type III*. J. Mech. Sci. . Technol. **29**(2015), 3739–3746.

[18] Abd-Alla A.M., Abo-Dahab S.M., Alotabi Hind A.: *Propagation of a thermoelastic wave in a half-space of a homogeneous isotropic material subjected to the effect of gravity field*. Arch. Civil and Mech. Eng. **17**(2017), 564–573.

[19] Abd-Alla A.M., Abo-Dahab S.M., Khan A.: *Rotational effect on thermoelastic Stoneley, Love and Rayleigh waves in fibre-reinforced anisotropic general viscoelastic media of higher order*. Struct. Eng. Mech. **61**(2017), 221–230.

[20] Puri P.: *Plane waves in thermoelasticity and magneto-thermoelasticity*. Int. J. Eng. Sci. **10**(1972), 467–477.

[21] Abo-Dahab S.M., Abd-Alla A.M., Alotabi Hind A.: *On influence of thermal stress and magnetic field in thermoelastic half-space without energy dissipation*. J. Therm. Stresses **40**(2017), 213–230.

[22] Abd-Alla A.M., Mahmoud S.R.: *Magneto-thermoelastic problem in rotating non-homogeneous orthotropic hollow cylinder under the hyperbolic heat conduction model*. Meccanica **45**(2010), 451–462.

[23] Othman M.I.A.,Zidan M.E.M., Hilal M.I.M.: *2-D problem of a rotating thermoelastic solid with voids under thermal loading due to laser pulse and initial stress type III*. J. Therm. Stresses **38**(2015), 835–853.

[24] Othman M.I.A.,Hasona W.M., Abd-Elaziz E.M.: *The influence of thermal loading due to laser pulse on generalized micropolarthermoelastic solid with comparison of different theories*. Multidiscip. Model. Mater. Struct. **10**(2014), 328–345.

[25] Dhaliwal R.S., Singh A.: *Dynamic Coupled Thermoelasticity*. Hindustan Pub. Corp., New Delhi (1980).

[26] Marin M.: *A temporally evolutionary equation in elasticity of micropolar bodies with voids*. Appl. Math. Phys. **60**(1998), 3–12.

[27] Marin M., Stan G.: *Weak solutions in Elasticity of dipolar bodies with stretch*. Carpathian J. Math. **29**(2013), 1, 33–40.

[28] Marin M., and Baleanu D.: *On vibrations in thermoelasticity without energy dissipation for micropolar bodies*. Boundary Value Problems **111**(2016), 1–19.